Available online at www.sciencedirect.com
ScienceDirect
Journal of Solid State Chemistry 180 (2007) 167–172
JOURNAL OF SOLID STATE CHEMISTRY
www.elsevier.com/locate/jssc

Mild hydrothermal synthesis and magnetic properties of the manganates $Pr_{1-x}Ca_xMnO_3$

Yan Chen, Hongming Yuan, Ge Tian, Ganghua Zhang, Shouhua Feng*

State Key Laboratory of Inorganic Synthesis and Preparative Chemistry, College of Chemistry, Jilin University, Changchun 130023, PR China

Received 13 July 2006; received in revised form 12 September 2006; accepted 17 September 2006
Available online 10 October 2006

Abstract

The calcium-doped manganates, $Pr_{1-x}Ca_xMnO_3$ ($x = 0.39, 0.46, 0.70, 0.76$), were synthesized as cube-shaped crystalline phases under mild hydrothermal conditions for the first time. The crystals could be grown in one step from solutions of metal salts and potassium hydroxide at temperatures ~240 °C, and found to adopt perovskite-like structure (space group *Pbnm*). Samples were characterized by powder X-ray diffraction, scanning electron microscopy, inductively coupled plasma analysis and variable temperature dc/ac magnetic susceptibility. The studies indicate that formation of the materials is dependent on the alkalinity and composition of the initial reaction mixtures. The magnetic properties show spin-glass-like behavior due to competing ferromagnetic (FM) and antiferromagnetic (AFM) exchange interactions in $Pr_{1-x}Ca_xMnO_3$ with $x = 0.39, 0.46$.

Keywords: Hydrothermal; Manganate; Spin-glass-like

1. Introduction

The perovskites $R_{1-x}A_xMnO_3$ (where R is a trivalent lanthanide cation and A is a divalent alkali-earth cation), have stimulated intense interest in recent years, on account of their useful magnetic and electronic properties [1–4]. In the $LaMnO_3$ system, partial substitution of Ca^{2+} for La^{3+} leads to the formation of mixed valence at the Mn-site (Mn^{3+} and Mn^{4+}), which gives rise to colossal magnetoresistance (CMR) effect via the Double-Exchange (DE) mechanism [5–7]. Magnetic and electric transport properties of the materials are affected by adjusting the doping divalent or trivalent cations. The smaller ion size Pr^{3+} in comparison to La^{3+} in the perovskite-like structure induces a larger lattice distortion because of the tolerance factor considerations. In fact, the ionic radius of R^{3+} and A^{2+} determines the one-electron bandwidth and charge order (CO) is observed in $Pr_{1-x}Ca_xMnO_3$ system with small ionic radius of Pr^{3+} and Ca^{2+}. The charge-ordering phenomenon is reported to persist over a large composition range of $0.3 < x < 0.9$ [8]. Furthermore, manganates $Pr_{1-x}Ca_xMnO_3$ show a transition to an electrically insulating charge-ordered state from a metallic ferromagnetic (FM) state around $x = 0.3$. It shows canted FM structure accompanied with antiferromagnetic (AFM) ground state of a CE-type structures.

Perovskite-based lanthanide manganates are usually prepared by traditional high temperature solid-state methods, which require calcination of oxide/carbonate/nitrate precursors at temperatures in excess of 1000 °C with frequent grindings [9–11]. Although these methods are adequate for the synthesis of X-ray pure specimens, it is often difficult to control the total oxygen content in the mixed valence systems because of the high temperatures used in the synthesis. Soft chemical methods, such as the use of sol–gel precursors or molten salts as reaction media, have been adopted for the synthesis of oxide, but these methods involve often complex operating procedures. Hydrothermal technique has been widely applied to the synthesis of metastable phases and microporous solids [12]. This method provides an attractive alternative to the synthesis of complex oxides and fluorides, since it is carried out under relatively mild conditions (autogeneous pressure

*Corresponding author. Fax: +86 431 516 8624.
E-mail address: shfeng@mail.jlu.edu.cn (S. Feng).

0022-4596/$ - see front matter © 2006 Elsevier Inc. All rights reserved.
doi:10.1016/j.jssc.2006.09.029

and ~240 °C) with controllable particle size distribution of the product [13–15]. Mild hydrothermal methods have been used for the preparation of perovskite materials [16,17]. Spooren et al. have reported the synthesis of polycrystalline compositions, $R_{0.5}A_{0.5}MnO_3$ using hydrothermal methods [18–20]. Recently, we have demonstrated the feasibility of using the hydrothermal methods in the crystal growth of manganese oxide perovskites containing rare-earth ions [21]. So far, the applicability of hydrothermal methods to the synthesis of rare-earth manganates is limited to only compositions where the manganese valence is exclusively 3 or 3.5. To our knowledge, there are no reports on the synthesis of continuous solid solutions of the composition $R_{1-x}A_xMnO_3$ using hydrothermal means. Given the ease of hydrothermal synthesis, we have explored various compositional, temperature and pH conditions that might yield continuous solid solutions of the type $R_{1-x}A_xMnO_3$. As a part of these investigations, we report here the hydrothermal synthesis and magnetic properties of few Pr-based manganate compositions with the general formula $Pr_{1-x}Ca_xMnO_3$ ($0.4<x<0.75$). Our observations indicate that the successful synthesis of these X-ray Pure cube-shaped crystalline phases require careful control of the pH of the reactant mixture, temperature and choice of salts. We also report here their preliminary magnetic properties.

2. Experimental section

In a typical synthetic procedure for $Pr_{0.54}Ca_{0.46}MnO_3$, we prepared the parent solution using 10 mL $KMnO_4$ (0.12 M), 5 mL $Pr(NO_3)_3$ (0.4 M) and 5 mL $Ca(NO_3)_2$ (0.4 M) and 20 g KOH. The resulting solution was stirred thoroughly prior to the addition of 5 mL $MnCl_2$ (0.56 M) ($MnSO_4$ was used in some preparations). The mixture was then transferred into a 50-mL Teflon-lined stainless-steel autoclave to a filling capacity of 80%. Crystallization was carried out under autogenous pressure at 240 °C for 3 days. After the autoclave was cooled and depressurized, the product in the form of black crystalline powder was washed thoroughly with distilled water and sonicated. The reaction conditions employed for the synthesis of other compositions featuring various Pr/Ca ratios are listed in Table 1. The contents of manganese, praseodymium and calcium in the final products were determined by inductively coupled plasma spectrosometer (Medac Ltd.).

Powder X-ray diffraction (XRD) data were collected using a Rigaku D/Max 2500 V/PC X-ray diffractometer with Cu$K\alpha$ radiation ($\lambda = 1.5418$ Å) at 40 kV and 200 mA at room temperature by step scanning in the angle range of $5^\circ \leqslant 2\theta \leqslant 120^\circ$ using increments of 0.02°. Scanning electron microscope (SEM) images were taken with a JEOL JSM-6700F microscope operating at 10 kV. The ac/dc magnetic susceptibilities were measured with a SQUID magnetometer (Quantum Design, MPMS-LX) at various applied magnetic fields and temperatures in the range 4–300 K.

3. Results and discussion

In the hydrothermal of $Pr_{1-x}Ca_xMnO_3$, it was found that the nature of the reactants, initial composition and alkalinity in reaction mixtures dictate the formation, crystallinity and purity of the products. In order to adjust the doping level (x) in $Pr_{1-x}Ca_xMnO_3$, it is necessary to have the appropriate molar ratio of the initial reactants as shown in Table 1. A simplified redox reaction between MnO_4^- and Mn^{2+} (shown below) may be facilitated by the strong alkalinity of the solution used in our experiment:

$$(3+x)\mathrm{Mn(II)} + (2-x)\mathrm{Mn(VII)} \rightarrow 5\mathrm{Mn(III)}_{1-x}\mathrm{Mn(IV)}_x$$

We can get the precise mixed valence of manganese in the product $Pr_{1-x}Ca_xMnO_3$ through adjusting the ratio of $MnO_4^-/\ Mn^{2+}$ in the initial mixture. It has been reported that the redox reactions between the MnO_4^- and Mn^{2+} ions may result in an amorphous birnessite-like precursor, which has an octahedral layer (OL-1) structure [22]. In this structure, the metal ions and the water molecules located in the interlayer space of the mixed-valent manganese framework (MnO_6 octahedra) show strong activity in hydrothermal conditions. We propose that formation of the crystals is mediated by Birnessite-like precursor that forms when Mn^{2+} reacts with MnO_4^- under hydrothermal conditions because of the similarity of the Mn–O framework of birnessite and perovskite structures. Our results also indicate that any deviations from the prescribed $MnO_4^-/\ Mn^{2+}$ ratio always lead to the formation of impurity phase $K_{0.5}Mn_2O_4 \cdot 1.5H_2O$ [15,20].

In addition to the appropriate ratio of $MnO_4^-/\ Mn^{2+}$ in the starting solution, high alkalinity is also necessary for the crystallization of the products. As shown in Table 1, the amount of KOH required for the hydrothermal reaction varies with the target composition. In our experiment, samples with higher Ca/Pr ratio often required higher alkalinity. Although the precise role of base used in the synthesis of manganates is not clear, it is likely that high

Table 1
Product composition, initial reactant ratio and reaction temperature

Product composition temperature/°C	Molar ratio $Pr(NO_3)_3$: $Ca(NO_3)_3$: $KMnO_4$: $MnSO_4$	KOH concentration/M	Reaction
$Pr_{0.24}Ca_{0.76}MnO_3$	2.0: 8.0: 3.6: 6.4	17	240 °C
$Pr_{0.30}Ca_{0.70}MnO_3$	3.0: 7.0: 3.4: 6.6	14	240 °C
$Pr_{0.54}Ca_{0.46}MnO_3$	5.0: 5.0: 3.0: 7.0	13	240 °C
$Pr_{0.61}Ca_{0.39}MnO_3$	6.0: 4.0: 2.8: 7.2	11	240 °C

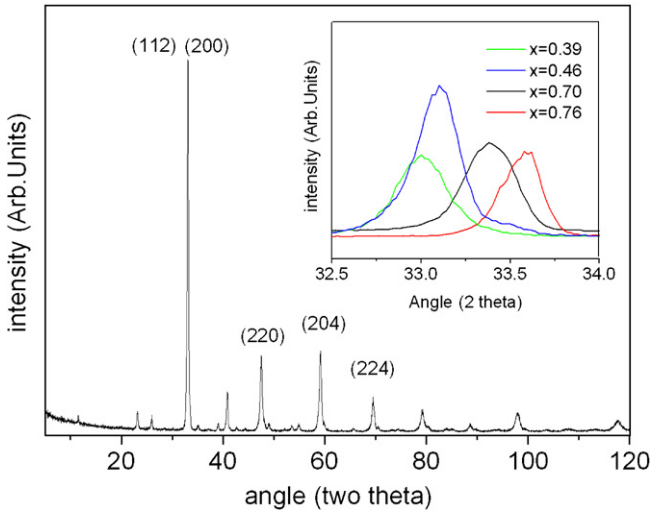

Fig. 1. XRD pattern for the manganate $Pr_{1-x}Ca_xMnO_3$($x = 0.46$).The inset shows (112, 200) diffraction peaks of the samples corresponding to the remaining four compositions($x = 0.39$, 0.46, 0.70, and 0.76), illustrating small and definite increase in lattice parameter as a function of calcium doping.

alkalinity favor the stabilization of tetra-valent manganese required for higher Ca/Pr ratio. It is also noteworthy that high alkalinity was essential to the synthesis of perovskite-type compounds such as $LnCrO_3$, $BiFeO_3$ and doped manganates $R_{0.5}A_{0.5}MnO_3$ by hydrothermal methods [23–25,31,32].

The room-temperature powder X-ray diffraction patterns for $Pr_{1-x}Ca_xMnO_3$ ($x = 0.39$, 0.46, 0.70, 0.76) are shown in Fig. 1. The XRD data could be indexed on the basis of known orthorhombic perovskite structure (S.G. = *Pbnm*). As shown in Table 2, the unit cell volume gradually increases as the calcium content decreases, which is also seen in the systematic shifts in the peak positions in the XRD patterns (see Fig. 1 inset). Such a monotonous increase is consistent with the difference between the ionic radii of Mn^{4+} and Mn^{3+} and size differences between the Pr^{3+} and Ca^{2+} ions.

It appears that higher alkalinity favors crystallinity in the $Pr_{1-x}Ca_xMnO_3$ system as shown in Fig. 2. It is clear from these micrographs that the quality of the crystals gets better when the Ca/Pr ratio is relatively high. We have also

Table 2
Unit cell parameters of the manganates $Pr_{1-x}Ca_xMnO_3$ (*pbnm*)

Composition	*a*(Å)	*b*(Å)	*c*(Å)	*V*(Å^3)
$Pr_{0.24}Ca_{0.76}MnO_3$	5.33467±0.00194	5.34269±0.00163	7.53638±0.00255	214.79(8)
$Pr_{0.30}Ca_{0.70}MnO_3$	5.33919±0.00311	5.34829±0.00275	7.59530±0.00381	216.88(8)
$Pr_{0.54}Ca_{0.46}MnO_3$	5.40337±0.00220	5.41343±0.00232	7.61674±0.00320	222.79(5)
$Pr_{0.61}Ca_{0.39}MnO_3$	5.42236±0.00210	5.43694±0.00216	7.68672±0.00310	226.61(3)

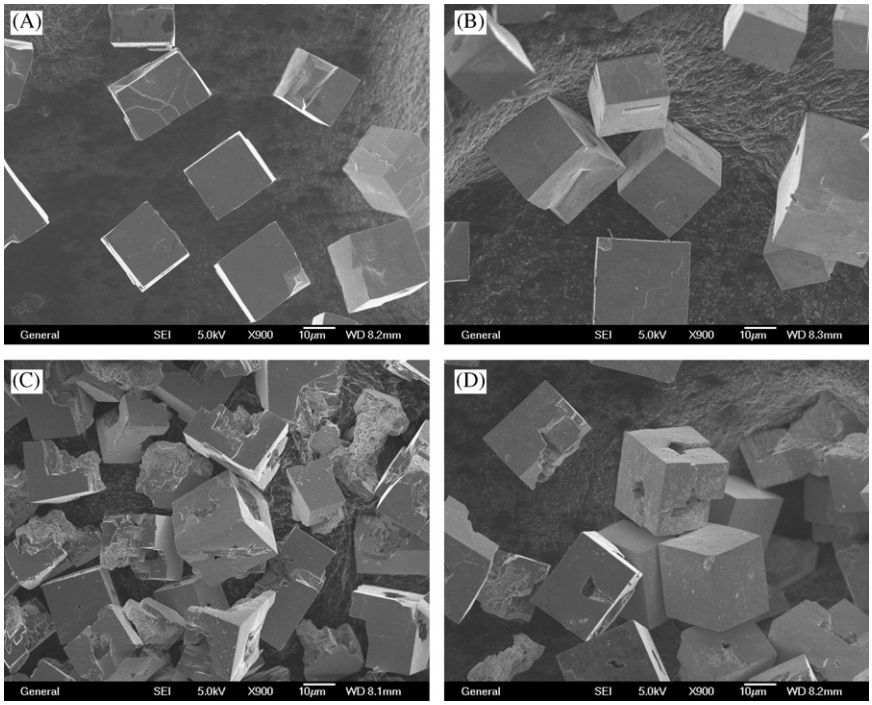

Fig. 2. SEM image of $Pr_{0.24}Ca_{0.76}Mn_3$ (A), $Pr_{0.30}Ca_{0.70}MnO_3$ (B), $Pr_{0.54}Ca_{0.46}MnO_3$(C), $Pr_{0.61}Ca_{0.39}MnO_3$ (D).

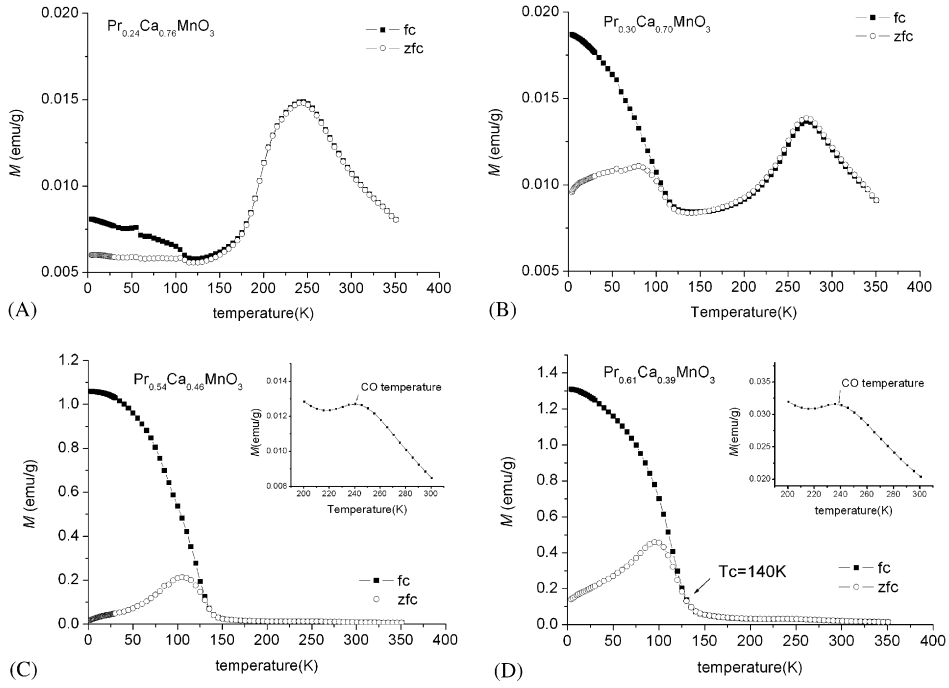

Fig. 3. Zero-field cooled (ZFC) and field cooled (FC) magnetization curves of manganates $Pr_{1-x}Ca_xMnO_3$ (A: $x = 0.76$, B: $x = 0.70$, C: $x = 0.46$, D: $x = 0.39$) in an applied field of 100 Oe. The inset in C and D show CO temperature is 240 K for the manganates $Pr_{1-x}Ca_xMnO_3$($x = 0.39$, 0.46).

carried out the hydrothermal synthesis using various salts of manganese and find that phase formation is favored with $MnSO_4$ in most cases. Interestingly however, the manganate $Pr_{0.54}Ca_{0.46}MnO_3$ can only be synthesized successfully when $MnCl_2$ was used as Mn(II) source. We also observe that higher temperatures lead to a better crystallization of the products. Samples with lower Ca-content ($x < 0.4$) could not be obtained under our experimental conditions, because higher molar concentration of $Pr(NO_3)_3$ gave rise to the formation of crystalline $Pr(OH)_3$, which is stable and remained in the final product.

In Fig. 3 we show the temperature dependence of the zero field cooled (ZFC) and field cooled (FC) magnetization at a magnetic field of 100 Oe for the series $Pr_{1-x}Ca_xMnO_3$ compounds. Broad down turns in the magnetization ~250 K for $x = 0.70$ and 0.76 results from well-known CO effects, followed a transition to AFM state below ~110 K. On the other hand, the manganates, $Pr_{0.54}Ca_{0.46}MnO_3$ and $Pr_{0.61}Ca_{0.39}MnO_3$, exhibit a sharp increase below a critical temperature in the magnetization curve, which may result from competing FM and AFM interactions. The critical temperatures were about 145 K for $Pr_{0.54}Ca_{0.46}MnO_3$ and 140 K for $Pr_{0.61}Ca_{0.39}MnO_3$.

Fig. 4 shows the isothermal magnetization curves of all the manganates studied here. From the plots it is clear that the FM phase was observed only in samples with low doping level ($x = 0.39$, 0.46). It is also clear that the highest magnetic field of 50 kOe (the highest in our SQUID magnetometer) is too low to saturate the magnetization. A small hysteresis is observed in $Pr_{0.54}Ca_{0.46}MnO_3$ and $Pr_{0.61}Ca_{0.39}MnO_3$ at low temperatures.

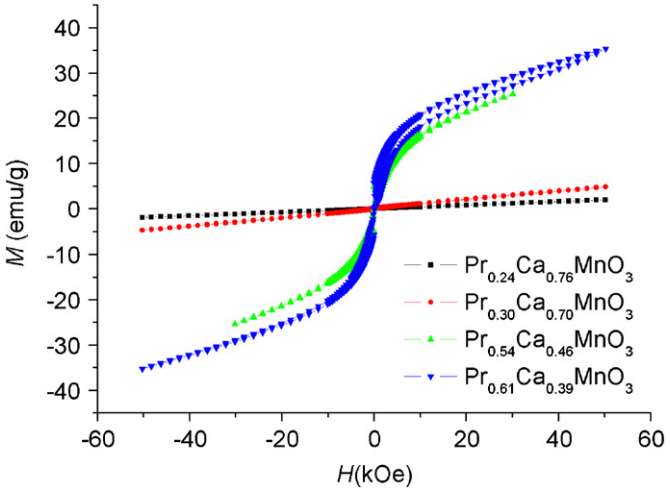

Fig. 4. Isothermal magnetization curves of the manganates $Pr_{1-x}Ca_xMnO_3$ ($x = 0.39$, 0.46, 0.70, 0.76) at 4 K.

Fig. 5 shows the ac susceptibility versus temperature behavior of $Pr_{0.54}Ca_{0.46}MnO_3$ and $Pr_{0.61}Ca_{0.39}MnO_3$ crystals at various frequencies. The real part, χ', increases rapidly near the onset of the magnetic ordering temperature, and decreases upon further cooling. A maximum value was observed at 105 K, which coincidences well with the dc measurement. We also observe that both the real and imaginary susceptibilities are frequency dependent in the temperature range of 4–140 K. Detectable shift of maximum in the real part of the susceptibility can be observed with the increase of the frequency in $\chi'(T)$ which

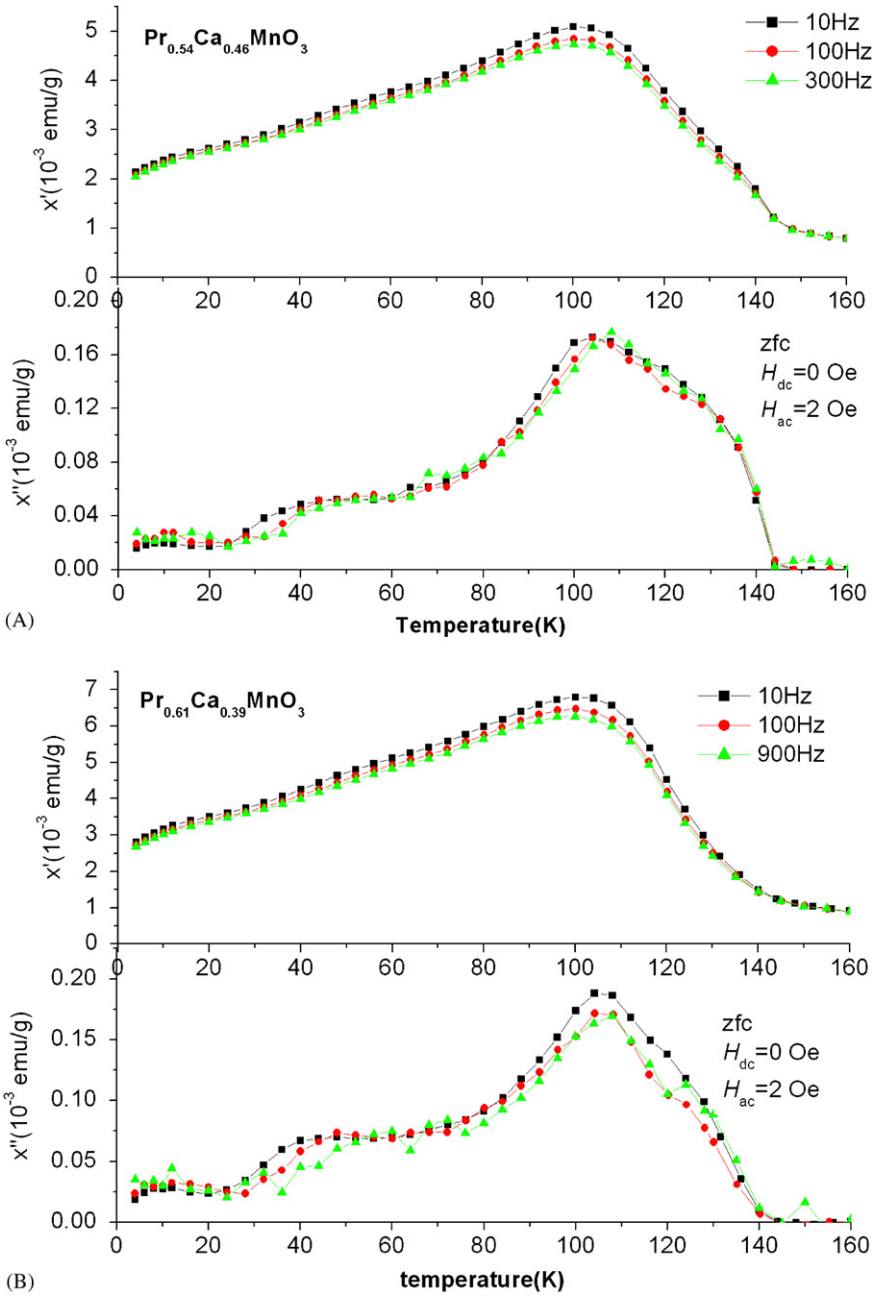

Fig. 5. The temperature dependence of the real and imaginary component of the ac susceptibility for the A: $Pr_{0.54}Ca_{0.46}MnO_3$ B: $Pr_{0.61}Ca_{0.39}MnO_3$ samples at different frequencies.

suggests the presence of either spin-glass or cluster-glass behavior. These observations are somewhat reminiscent of earlier reports on $Ca_{1-x}Sm_xMnO_3$, $La_{0.5}Sr_{0.5}CoO_3$ and $LaMnO_{3+\delta}$ [26–29] wherein the double-exchange interactions between M^{4+} and M^{3+} (M = Mn or Co) ions are reported to induce FM order, while the M^{3+}–M^{3+} and M^{4+}–M^{4+} interactions are AFM due to the superexchange interactions. Frustration may appear as a consequence of the coexistence or competition of AFM and FM interactions [30]. Hysteresis observed in $Pr_{0.61}Ca_{0.39}MnO_3$ and $Pr_{0.54}Ca_{0.46}MnO_3$ at low field also confirms the low-field glass-like nature of the samples and an evidence for a disordered spin state.

4. Conclusions

In summary, crystals of calcium-doped manganates $Pr_{1-x}Ca_xMnO_3$ ($x = 0.39$, 0.46, 0.70, 0.76) have been synthesized by mild hydrothermal method for the first time. The alkalinity, initial mole ratio of reactants in the mixture, temperature and source of manganese ions are found to influence the crystallization of the materials. Study on magnetic properties shows the spin-glass-like behavior at low temperature in the manganates $Pr_{0.54}Ca_{0.46}MnO_3$ and $Pr_{0.61}Ca_{0.39}MnO_3$. Crystals with high Ca/Pr ratio showed charge-ordering and anti-ferromagnetic transition at low temperatures.

Acknowledgments

We thank Professor K.V. Ramanujachary and Professor Tongyun Zhao for helpful discussion. This work was supported by the National Natural Science Foundation of China (No. 20121103 and 20301007).

Appendix A. Supplementary Materials

Supplementary data associated with this article can be found in the online version at doi:10.1016/j.jssc.2006.09.029.

References

[1] A. Asamitsu, Y. Moritomo, Y. Tomioka, T. Arima, Y. Tokura, Nature 373 (1995) 407.
[2] G.M. Zhao, K. Conder, H. Keller, K.A. Miiller, Nature 381 (1996) 676.
[3] G.H. Jonker, J.H. van Santen, Physica 16 (1950) 599.
[4] C. Zener, Phys. Rev. 82 (1951) 403.
[5] J. Inoue, S. Maekawa, Phys. Rev. Lett. 74 (1995) 3407.
[6] J.H. Kuo, H.U. Anderson, D.M. Sparlin, J. Solid State Chem. 83 (1989) 52.
[7] N. Shannon, A.V. Chubukov, J. Phys.: Condens. Matter. 14 (2002) 235.
[8] M. Lees, J. Barratt, G. Balakrishnan, D.M. Paul, Phys. Rev. B. 52 (1995) R14303.
[9] J. Tanaka, K. Takahashi, Y. Yajima, M. Tsukioka, Chem. Lett. (1992) 1847.
[10] B. Dabrowski, R. Dybzinski, Z. Bukowski, O. Chmaissem, J.D. Jorgensen, J. Solid State Chem. 146 (1999) 448.
[11] J.-S. Zhou, J.B. Goodenough, Phys. Rev. B. 68 (2003) 144406.
[12] S.H. Feng, R.R. Xu, Acc. Chem. Res. 34 (2001) 239.
[13] R. Yu, F. Xiao, D. Wang, J. Sun, Y. Liu, G. Pang, S. Feng, S. Qiu, R. Xu, S. Ma, Catal. Lett. 49 (1997) 49.
[14] Y. Zhang, H. Wang, B. Wang, H. Yan, A. Ahniyaz, M. Yoshimura, Mater. Res. Bull. 37 (2002) 1411.
[15] D. Wang, R. Yu, S. Feng, W. Zheng, R. Xu, N. Kumada, N. Kinomura, Mater. Res. Bull. 36 (2001) 239.
[16] D. Wang, R. Yu, S. Feng, W. Zheng, G. Pang, H. Zhao, Chem. J. Chin. Univ. 19 (1998) 165.
[17] D. Wang, R. Yu, S. Feng, W. Zheng, R. Xu, Y. Matsumura, M. Takano, Chem. Lett. 32 (2003) 74.
[18] J. Spooren, A. Rumplecker, F. Millange, R.I. Walton, Chem. Mater. 15 (2003) 1401.
[19] J. Spooren, R.I. Walton, F. Millange, J. Mater. Chem. 15 (2005) 1542.
[20] J. Spooren, R.I. Walton, J. Solid State Chem. 178 (2005) 1683.
[21] Y. Wang, X. Lu, Y. Chen, F. Chi, S. Feng, J. Solid State Chem. 178 (2005) 1317–1320.
[22] X.-F. Shen, Y.-S. Ding, J. Liu. J. Cai, K. Laubernds, R.P. Zerger, A. Vasiliev, M. Aindow, S.L. Suib, Adv. Mater. 17 (2005) 805.
[23] W. Zheng, W. Pang, G. Meng, D. Peng, J. Mater. Chem. 9 (1999) 2833.
[24] M. Wu, J. Long, G. Wang, A. Huang, Y. Luo, S. Feng, R. Xu, J. Am. Ceram. Soc. 82 (1999) 3254.
[25] Y. Shi, S. Feng, J. Li, C. zhang, W. Li, Chem. J. Chin. Univ. 20 (1999) 172.
[26] A. Maignan, C. Martin, F. Damay, B. Raveau, J. Heitmanek, Phys. Rev. B. 58 (1998) 2758.
[27] S. Mukherjee, R. Ranganathan, P.S. Anilkumar, P.A. Joy, Phys. Rev. B. 54 (1996) 9267.
[28] D.H.N. Nam, K. Jonason, P. Nordblad, N.V. Khiem, N.X. Phuc, Phys. Rev. B. 59 (1999) 4189.
[29] L. Ghivelder, I. Abrego Castillo, M.A. Gusmao, J.A. Alonso, L.F. Cohen, Phys. Rev. B. 60 (1999) 12184.
[30] L. Sudheendraa, A.R. Raju, S.E. Lofland, K.V. Ramanujachary, Solid State Commun. 126 (2003) 447.
[31] C. Zhao, S. Feng, R. Xu, C. Shi, J. Ni, Chem. Commun. 945 (1997) 8.
[32] Y. Mao, G. Li, W. Xu, S.J. Feng, Mater. Chem. 10 (2000) 479.